Report

Current Biology

Reinforcement learning links spontaneous cortical dopamine impulses to reward

Graphical abstract

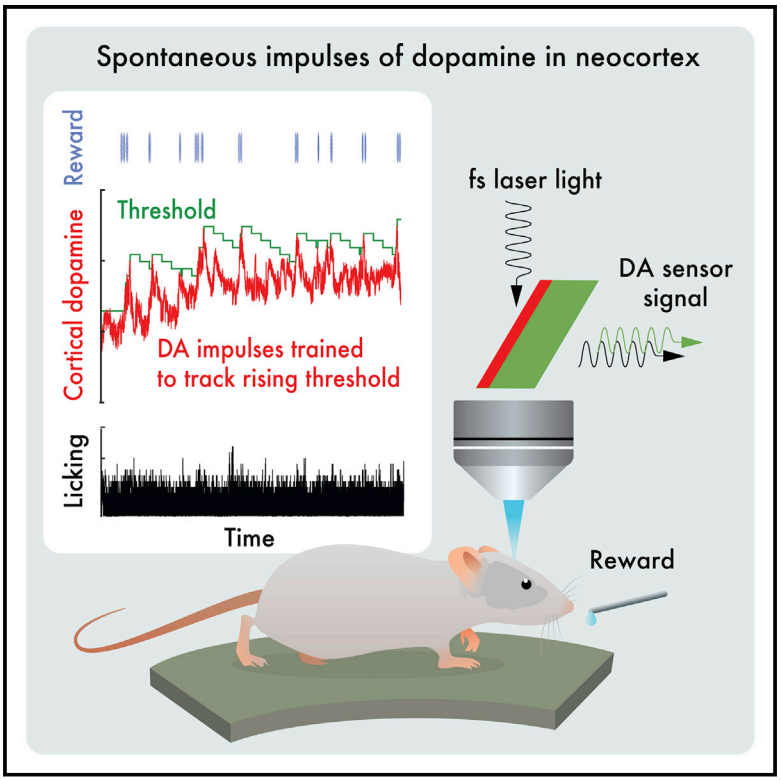

Highlights

- Extrasynaptic levels of dopamine in mouse cortex exhibit spontaneous impulses
- Impulses are broadly distributed in amplitude and time, with a rate of about 0.01/s
- Feedback was used to train mice to volitionally control their spontaneous impulses
- Mice learned to reliably modulate dopamine impulses in order to receive a reward

Authors

Conrad Foo, Adrian Lozada, Johnatan Aljadeff, Yulong Li, Jing W. Wang, Paul A. Slesinger, David Kleinfeld

Correspondence

paul.slesinger@mssm.edu (P.A.S.), dk@physics.ucsd.edu (D.K.)

In brief

Foo et al. found that spontaneous impulses of dopamine release occur in cortex of naive mice at a rate of ~0.01 per second. Using a reinforcement learning paradigm based on rewards that were gated by real-time measurements of extrasynaptic dopamine, mice could learn to volitionally modulate their spontaneous impulses.

Foo et al., 2021, Current Biology *31*, 4111–4119
September 27, 2021
https://doi.org/10.1016/j.cub.2021.06.069

CellPress

Current Biology

CellPress

Report

Reinforcement learning links spontaneous cortical dopamine impulses to reward

Conrad Foo,[1] Adrian Lozada,[1] Johnatan Aljadeff,[2] Yulong Li,[3] Jing W. Wang,[2] Paul A. Slesinger,[4,5,*] and David Kleinfeld[1,2,6,*]

[1]Department of Physics, University of California at San Diego, La Jolla, CA 92093, USA
[2]Section of Neurobiology, University of California at San Diego, La Jolla, CA 92093, USA
[3]Peking University, School of Life Sciences, Peking University, Beijing 100871, P.R. China
[4]Department of Neuroscience, Icahn School of Medicine at Mount Sinai, New York, NY, USA
[5]Twitter: @paslesin
[6]Lead contact
*Correspondence: paul.slesinger@mssm.edu (P.A.S.), dk@physics.ucsd.edu (D.K.)
https://doi.org/10.1016/j.cub.2021.06.069

SUMMARY

In their pioneering study on dopamine release, Romo and Schultz speculated "...that the amount of dopamine released by unmodulated spontaneous impulse activity exerts a tonic, permissive influence on neuronal processes more actively engaged in preparation of self-initiated movements...."[1] Motivated by the suggestion of "spontaneous impulses," as well as by the "ramp up" of dopaminergic neuronal activity that occurs when rodents navigate to a reward,[2–5] we asked two questions. First, are there spontaneous impulses of dopamine that are released in cortex? Using cell-based optical sensors of extrasynaptic dopamine, $[DA]_{ex}$,[6] we found that spontaneous dopamine impulses in cortex of naive mice occur at a rate of ~0.01 per second. Next, can mice be trained to change the amplitude and/or timing of dopamine events triggered by internal brain dynamics, much as they can change the amplitude and timing of dopamine impulses based on an external cue?[7–9] Using a reinforcement learning paradigm based solely on rewards that were gated by feedback from real-time measurements of $[DA]_{ex}$, we found that mice can volitionally modulate their spontaneous $[DA]_{ex}$. In particular, by only the second session of daily, hour-long training, mice increased the rate of impulses of $[DA]_{ex}$, increased the amplitude of the impulses, and increased their tonic level of $[DA]_{ex}$ for a reward. Critically, mice learned to reliably elicit $[DA]_{ex}$ impulses prior to receiving a reward. These effects reversed when the reward was removed. We posit that spontaneous dopamine impulses may serve as a salient cognitive event in behavioral planning.

RESULTS

We measured extrasynaptic dopamine ($[DA]_{ex}$) in primary somatosensory (S1) cortex of mice, which is known to exhibit stimulus-dependent[10] and experience-dependent synaptic plasticity.[11] Extrasynaptic dopamine is converted into an optical signal by cell-based neurotransmitter fluorescent-engineered reporters (CNiFERs).[6] The CNiFERs are implanted into cortex and observed with *in vivo* two-photon microscopy[12] through a thin-skull craniotomy that minimizes neuroinflammation.[13] We chose this approach for a multitude of reasons. First, we wish to make a direct measurement at the site of action rather than infer release from the spiking output of dopaminergic neurons that project to S1 cortex.[14–16] This is particularly important in light of differences in somatic spiking and dopaminergic release.[17,18] Second, D2-CNiFERs leverage the specificity of D2 dopamine G-protein-coupled-receptors (GPCRs) and thus have physiological nanoMolar sensitivity for $[DA]_{ex}$.[6] This enables D2-CNiFERs to detect small changes in $[DA]_{ex}$ with high sensitivity and with fast temporal resolution, i.e., <0.25 s. The same approach of using GPCRs was taken with recent single-wavelength, molecular sensors.[19,20] Third, CNiFERs report a change in $[DA]_{ex}$ through dual-wavelength fluorescence resonant energy transfer (FRET), which is relatively insensitive to optical bleaching, drift, and motion of the head compared with single-wavelength detectors. In fact, we compared the use of a genetically encoded dopamine sensor, $GRAB_{DA}$, against that of the CNiFERs (Figure S1); while $GRAB_{DA}$ was more sensitive to fast transients, it did not have the long-term stability needed for the current experiments.

We began with open-loop measurements on naive mice that had no prior experience with the apparatus (7 mice). The animals were implanted with D2-CNiFERs below a thinned-skull optical window, allowed to recover, and studied under head-fixed conditions on a running disk (Figure 1A). For these naive animals, we observed spontaneous, transient increases, i.e., impulses, in $[DA]_{ex}$ (Figure 1B). Interestingly, there is negligible statistical coherence between changes in $[DA]_{ex}$ and the speed of locomotion (Figure 1C). As an average over all animals, spontaneous dopamine transients occur at a rate of 0.007 ± 0.001 Hz (mean ± SE; Figure 1D) or about once every 140 s. The peak amplitude of spontaneous impulses is distributed across roughly a 3-fold range of

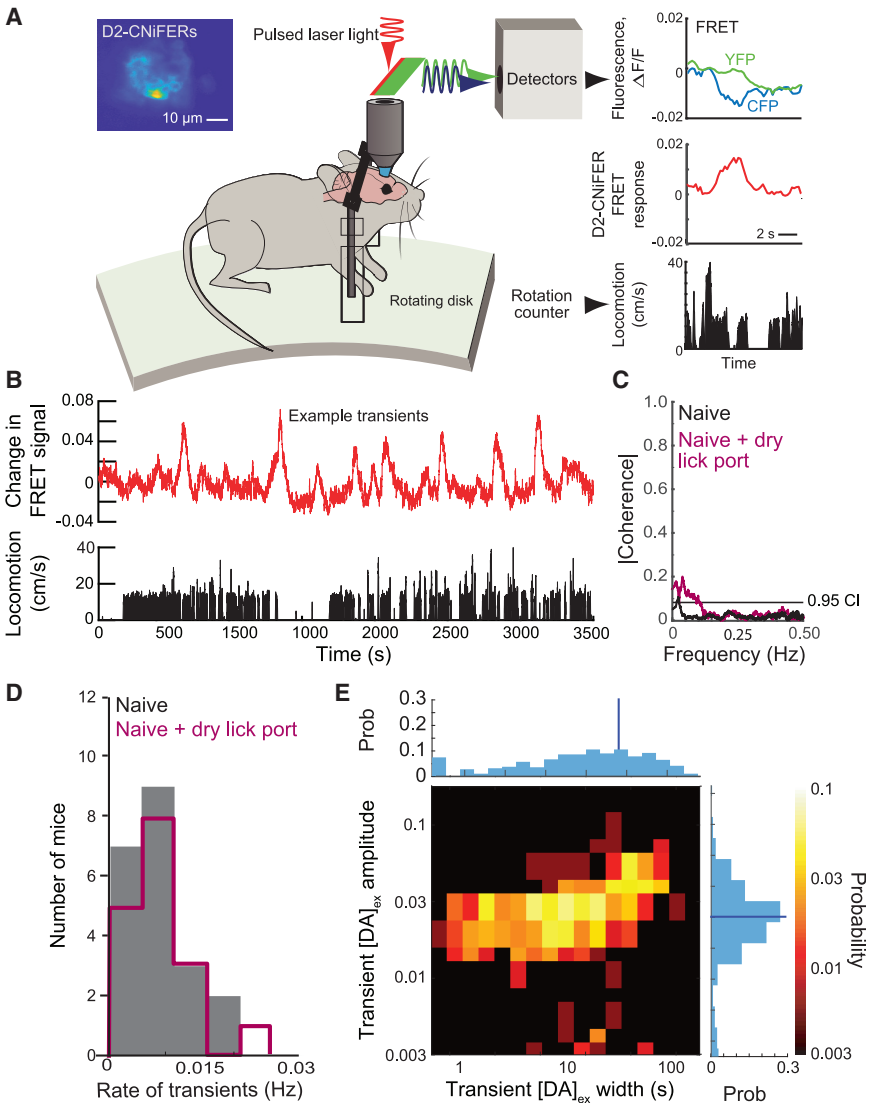

Figure 1. Characterization of spontaneous dopamine impulses ([DA]$_{ex}$) in naive mice in the absence of reward in an apparatus without a lick port or overt stimulation

(A) Open-loop measurement of cortical [DA]$_{ex}$ using D2-CNiFERs with *in vivo* two-photon microscopy. Increases in [DA]$_{ex}$ are observed as an increase in YFP fluorescence with a concomitant decrease in CFP fluorescence and vice versa. The CNiFER signal is reported as the fractional change in FRET.[21] Inset: fluorescence image of D2 CNiFER implant in cortex is shown.

(B) Time series shows changes in D2 CNiFER FRET, reflecting spontaneous transients in [DA]$_{ex}$, i.e., dopamine impulses, along with measurement of the rate of locomotion.

(C) The magnitude of the spectral coherence magnitude, averaged over all animals (xx mice), between the locomotion rate and [DA]$_{ex}$. Data without lick port in black and with dry port in maroon are shown; dashed line is 0.95 confidence level.

(D) Distribution of spontaneous dopamine impulse rate for all naive animals. Histograms without lick port (gray) and with port (maroon) are statistically indistinguishable (KS test; p = 0.99).

(E) Two-dimensional histogram of spontaneous impulses in [DA]$_{ex}$ across all animals without lick port. Top row is the cumulative of all widths; the average full width half maximum relative to baseline was 15.1 ± 1.3 s (blue line). Right column is the cumulative of amplitudes; 0.1 corresponds to [DA]$_{ex}$ ~20 nM;[6] the average was 0.056 ± 0.002 (blue line).

See also Figure S1.

values (Figure 1E). These values are far from the saturation level for dopamine binding by the CNiFERs and correspond to almost an order of magnitude range in [DA]$_{ex}$.[6] The lifetime of the impulses is near-uniformly distributed from 1 s in width up to 100 s with a mean value of 12 s (Figure 1E). We take 100 s as the operational break point between dopamine impulses and changes in basal [DA]$_{ex}$, which we refer to as tonic events. All told, these data support the presence of spontaneous [DA]$_{ex}$ impulses in cortex.

We next asked whether spontaneous [DA]$_{ex}$ events could be subject to volitional control. To address this, we designed an experiment with three sequential epochs: baseline (day 1), feedback "ON" (days 2 and 3), and feedback "OFF" (day 4). To determine the baseline [DA]$_{ex}$, we performed open-loop measurements with naive mice. These measurements are identical to the assay of spontaneous events (Figure 1A) but with the addition of a dry lick port (Figure 2A). In the feedback ON epoch, we introduced a closed-loop system for reinforcement training.[22,23] The mouse now received a sucrose-water drop reward through the lick port if there was an increase in [DA]$_{ex}$ above a threshold concentration; the determination was evaluated every 0.25 s (Figure 2A). Importantly, there was no external cue; mice were simply rewarded for elevations in cortical [DA]$_{ex}$. To motivate mice to actively increase the peak level of [DA]$_{ex}$, we incorporated an adaptive staircase algorithm,[24] analogous to a progressive ratio in classical conditioning, that was based on the [DA]$_{ex}$ level in the feedback loop. Increases in [DA]$_{ex}$ triggered a progressively higher threshold for reward, while the threshold was gradually lowered if [DA]$_{ex}$ was unchanged or decreased. In the feedback OFF epoch on day 4, the reward was omitted. Additional epochs of feedback ON and OFF were performed in a subset of mice.

We detect spontaneous impulses in [DA]$_{ex}$ in the absence of any reward, as seen in the example baseline data of Figure 2B (left panel). Transient increases in [DA]$_{ex}$ occurred with an average rate of 0.008 ± 0.001 Hz (18 mice), statistically indistinguishable from that of naive animals in the absence of a port (Figure 1D). Unlike the case without a lick port, however, running and changes in [DA]$_{ex}$ weakly but significantly co-fluctuated over long timescales (Figure 1C), although the tonic level of [DA]$_{ex}$ stayed relatively constant over the period of the trial (Figure 2C, day 1). Lastly, mice naturally lick the dry port such that [DA]$_{ex}$ and licking very weakly co-fluctuated. In total, these data confirm the presence of spontaneous [DA]$_{ex}$

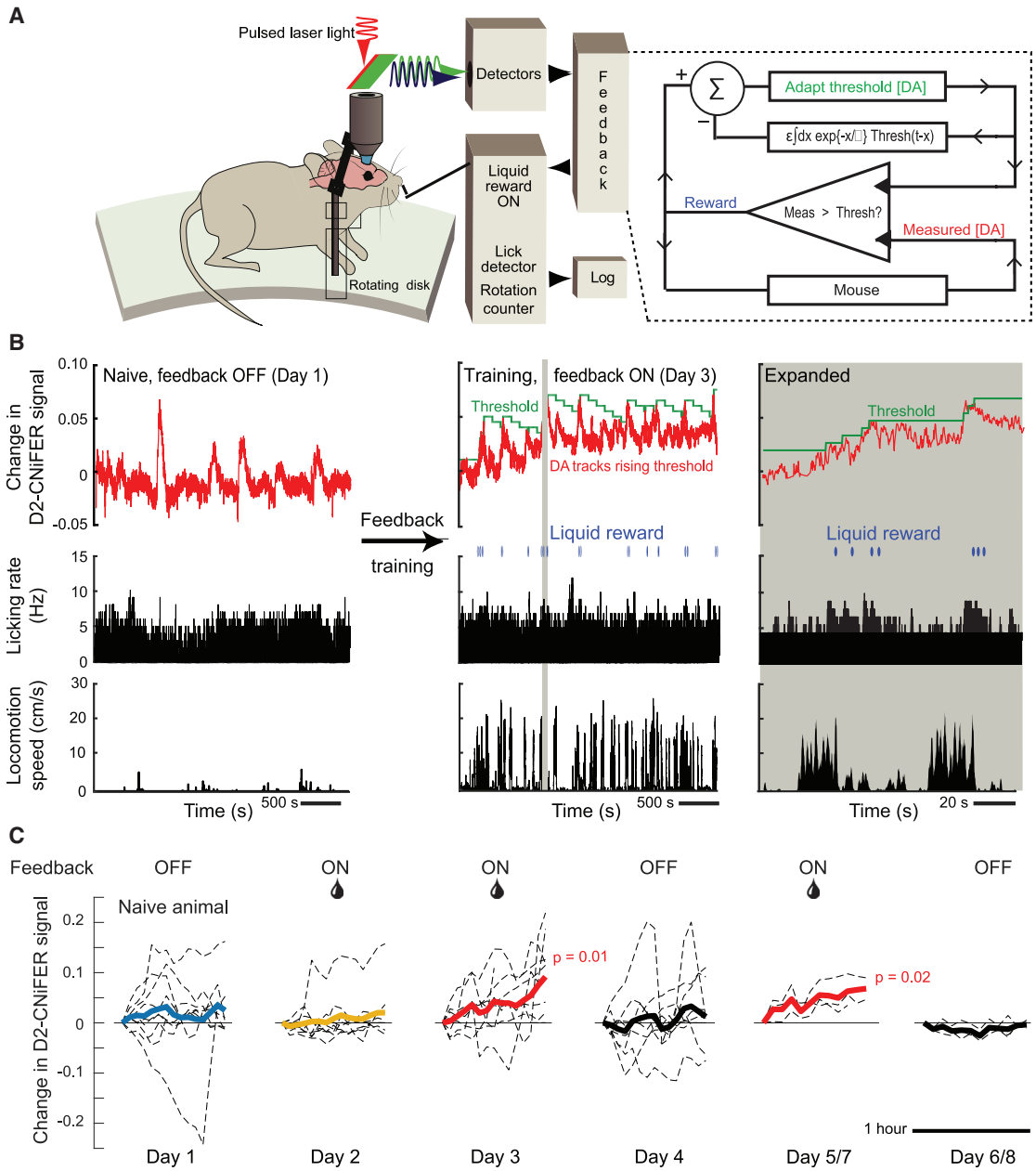

Figure 2. Closed-loop feedback reinforcement training to volitionally link spontaneous impulses in $[DA]_{ex}$ to reward

(A) The setup for the open loop experiment (Figure 1A) is augmented. We use the measured D2-CNiFER response as a proxy for $[DA]_{ex}$ and drive the delivery of a liquid reward based on the $[DA]_{ex}$ signal (red) relative to an adaptive staircase threshold (green) updated every 0.25 s. If $[DA]_{ex}$ exceeds the threshold, a drop (0.1 mL) of sucrose water (10% w/v) is released via the lick port and the threshold is incremented by 0.005 signal units. The value of the threshold also exponentially decreases, in discrete steps of 0.005, with a time constant of 225 s, since the last increment.

(B) Example data show the open-loop naive response on day 1 and an increase of tonic $[DA]_{ex}$ with closed-loop reinforcement on day 3; the adaptive staircase threshold follows the reward to within the decay time constant. A 130-s segment of data highlighted by the beige band is expanded.

(C) Rolling average of $[DA]_{ex}$ impulses for all mice. The averaging window was 235 s. On day 2, tonic $[DA]_{ex}$ did not significantly increase relative to that of naive mice ($p = 0.69$). By day 3, tonic $[DA]_{ex}$ increased significantly ($p = 0.01$). The increase extinguished when reward was withheld on day 4 ($p = 0.73$) and reinstated when reward was restored on day 5 or 7 ($p = 0.02$) compared to feedback withheld on day 6 or 8.

impulses in the baseline epochs and add to the results for naive animals (Figures 1A–1E).

On the 1st day of feedback training (9 mice), cortical $[DA]_{ex}$ remains essentially constant over the 1 h of ON training (Figure 2C, day 2). By contrast, the closed-loop reinforcement during the 2nd day of feedback ON training led to a large, statistically significant increase in $[DA]_{ex}$ over the period of training ($p = 0.01$; Figure 2C, day 3). As shown in the example of Figure 2B (center and right panels), mice tracked the increasing values of the threshold initiated by the adaptive staircase algorithm. Thus, the mice learned

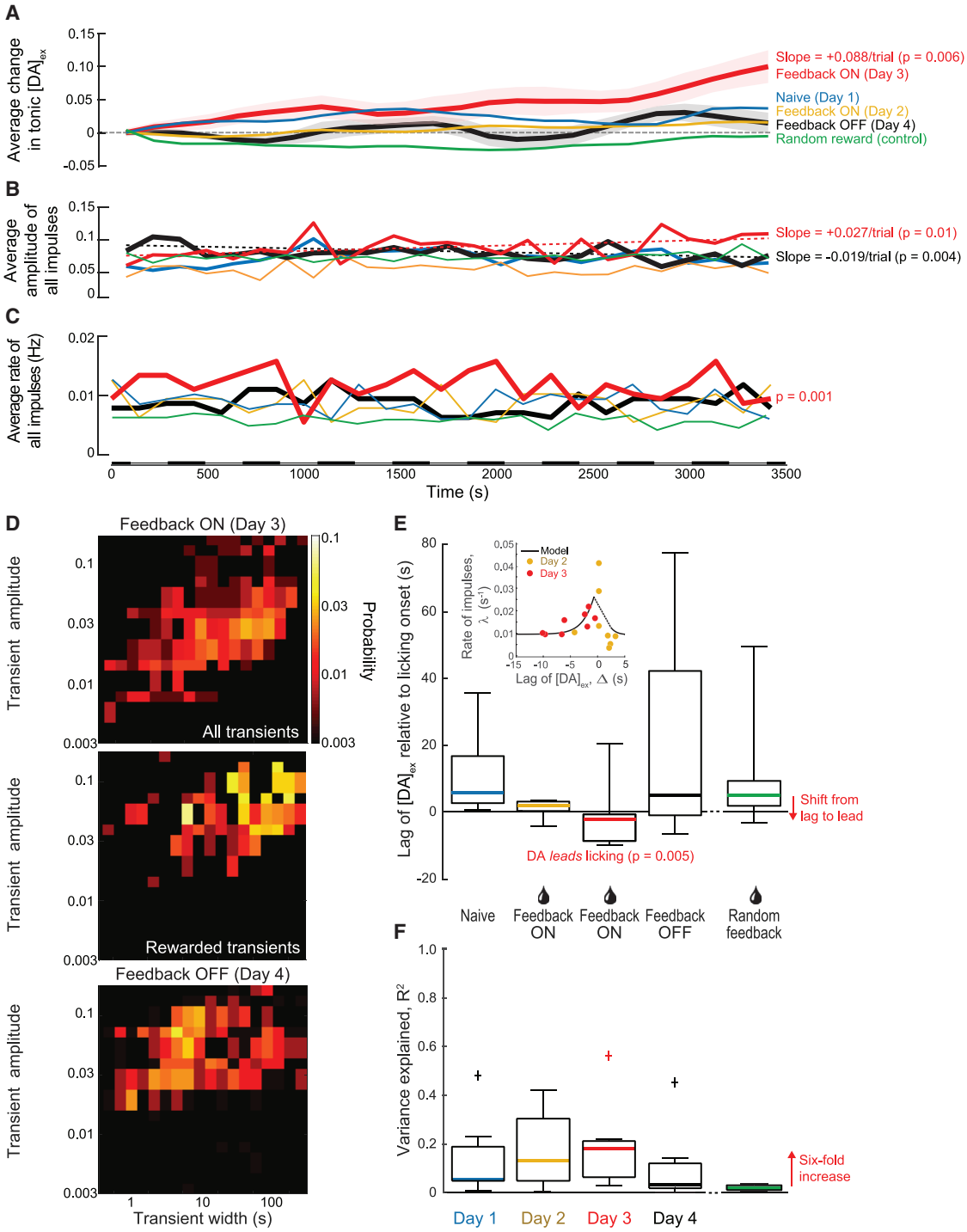

Figure 3. Population-averaged changes in $[DA]_{ex}$ over the course of our reinforcement paradigm

(A) Tonic $[DA]_{ex}$ shows a significant increase relative to naive, baseline animals after feedback training (day 3; $p = 0.006$); the increase is $\Delta[DA]_{ex} = 0.088$. Day 2 and day 4 showed no significant change in tonic $[DA]_{ex}$, $p = 0.37$ and 0.66, respectively. Randomly rewarded mice also did not show a significant change in tonic $[DA]_{ex}$ compared to naive animals ($p = 0.61$).

(B) The amplitude of $[DA]_{ex}$ impulses significantly increased over the course of the trial with feedback training (day 3; $p = 0.01$). With feedback OFF, there was a significant decrease in amplitude over the course of the trial (day 4; $p = 0.004$). The data for day 1 and day 2 and the case of random reward showed no significant change in $[DA]_{ex}$ impulse amplitude over time; $p = 0.43$, $p = 0.77$, and $p = 0.67$, respectively.

(C) The rate of $[DA]_{ex}$ impulses was significantly higher relative to baseline animals with feedback training (day 3; $p = 0.001$). Day 2 and day 4 showed no significant change in $[DA]_{ex}$ impulse frequency; $p = 0.65$ and 0.37, respectively. The rate for animals with random reward was significantly less than that for naive animals ($p = 10^{-8}$). Alternating bars along time axis indicate intervals for binned data in (A)–(C).

(legend continued on next page)

to augment their $[DA]_{ex}$ by approximately 10% on day 2 relative to the beginning of the session for this example. Remarkably, the increase in tonic $[DA]_{ex}$ was abolished by disabling the reward, i.e., feedback OFF epoch, subsequent to the 2 days of training (Figure 2C, day 4). To confirm that learning to volitionally control $[DA]_{ex}$ was not extinguished by a single session of no reward (3 mice), we restored feedback ON training and reward on the next day (day 5) and observed a significant increase in $[DA]_{ex}$ ($p = 0.02$), similar to that on day 3. This increase in tonic $[DA]_{ex}$ was again absent when feedback was omitted on day 6 (Figure 2C, days 5 and 6). Taken together, these results imply that learning is effective and that mice can volitionally control their cortical $[DA]_{ex}$ when provided with feedback via an immediate reward.

The feedback-driven increase in $[DA]_{ex}$ consists of a slowly increasing tonic level peppered with transient dopamine impulses (Figure 2B, middle and right panels). We decomposed the response into tonic and transient components. On the 2nd day with feedback training (day 3), we observed a statistically significant ($p = 0.006$) and approximately monotonic increase in the tonic level of $[DA]_{ex}$ compared to the relatively flat level in naive mice (Figure 3A). There was no significant change in $[DA]_{ex}$ for the feedback OFF epochs. We examined two aspects of the $[DA]_{ex}$ impulses. First, we find that the amplitude of the impulses significantly increases ($p = 0.01$), by a factor of 0.27/1.00 or approximately 1/3 that of the tonic increase, over the time of the trial (Figure 3B). There was a significant decrease ($p = 0.01$) in the amplitude of the impulses for the feedback OFF epochs (Figure 3B). Second, we observed a small but significant increase ($p = 7 \times 10^{-5}$) in the frequency of dopamine impulses across subjects (Figure 3C). Here, there was no significant change for the feedback OFF epochs. These reversible changes in both the tonic level of $[DA]_{ex}$ and the impulses signify the importance of the feedback reward training during the session.

Feedback-driven impulses of $[DA]_{ex}$ last 43 s on average, significantly longer than events in the naive mouse (12 s; $p = 10^{-28}$; cf. Figures 1E and 3D) or when feedback was removed ($p = 10^{-15}$; Figure 3D), but well within the 100-s operational definition of dopamine impulses.

An increase in the tonic level of $[DA]_{ex}$ could, in principle, result from the summation of multiple, slow, transient events. This possibility is unlikely for several reasons. First, in numerical tests of this possibility, we found that integration of dopamine impulses against a range of slow temporal filters, with decay times from 100 to 1,000 s, does not lead to a result with the observed increase in tonic level of $[DA]_{ex}$ (Figures S2A and S2B). Second, a tonic increase in $[DA]_{ex}$ is not observed with random rewards or on day 1 of reinforcement.

Could mice have associated an unknown systematic cue from our experimental setup? To address this, we examined in a separate cohort of mice (3 animals) the effect of rewarding at random intervals during the 1-h training on days 2 and 3 (Figure 2C). Random rewards were delivered following a Poisson distribution at a rate equal to the mean frequency of transients in $[DA]_{ex}$, i.e., 0.017 Hz, for mice trained on feedback. Mice that received rewards at random times did not show an increase in tonic $[DA]_{ex}$ or in the frequency, amplitude, or width of $[DA]_{ex}$ transients (Figures 3A–3C), in comparison with naive mice over the same time period (Figures S2C and S2D). Importantly, the onset of licking did not correlate with increases in $[DA]_{ex}$ (Figure 3E). Lastly, the extent of locomotion (Figures 1B and 2B), which has no overt function in the learning paradigm, is poorly predicted by $[DA]_{ex}$ (Figure S3), consistent with an incidental role.

Changes in timing of dopamine release are a hallmark of dopamine reinforcement learning. In classical reinforcement learning with liquid rewards, anticipatory licking is triggered by the conditioned stimulus, i.e., cue. However, in our experiments, there is no overt cue. Nonetheless, a critical test is to determine whether animals alter the timing of their dopamine dynamics with training. The expectation is that impulses of $[DA]_{ex}$ will occur prior to a reward after training, as opposed to following a reward. Indeed, we found this timing of $[DA]_{ex}$ impulses relative to the onset of licking shifts over the course of training. Naive mice naturally lick the dry port such that $[DA]_{ex}$ and licking weakly co-fluctuated with the increase in $[DA]_{ex}$, lagging that of licking by 11.0 ± 3.5 s (Figure 3E). In contrast, with feedback ON, the timing of the onset of dopamine has significantly advanced; $p = 0.04$ and $p = 0.005$ for days 2 and 3, respectively. For day 3, the advance is by 16 s, with the onset of $[DA]_{ex}$ impulses now occurring ahead of licking, i.e., lag of −5.1 ± 1.4 s (Figure 3E). Thus, feedback reinforcement reversed the temporal order of $[DA]_{ex}$ impulses and licking in trained mice so that the enhanced dopamine signal now predicts the outcome of a movement, i.e., licking.

In addition to changes in timing, we calculated the predictability of licking by $[DA]_{ex}$ under all conditions in terms of

(D) Distribution of amplitudes and widths of $[DA]_{ex}$ impulses for trained mice with feedback ON (day 3; top), a subset of rewarded impulses when feedback is ON (day 3; center), and when feedback reinforcement is OFF (day 4; bottom). The amplitudes with feedback training ON were significantly larger compared to baseline animals (day 3; $p = 10^{-7}$) and compared to feedback OFF (day 4; $p = 10^{-29}$). The widths were significantly greater with feedback ON compared to those for baseline animals ($p = 10^{-22}$) and when feedback was OFF ($p = 10^{-15}$). Rewarded impulses had an amplitude of 0.078 ± 0.002 and an average width of 44.2 ± 1.6 s and were significantly greater than the impulses when feedback was OFF (day 4; $p = 10^{-8}$ and $p = 10^{-29}$, respectively).

(E) Standard boxplot shows the timing of the onset of $[DA]_{ex}$ impulses relative to the onset of licking; the solid bars are the median times. The mean and standard error of the lag times of $[DA]_{ex}$ impulses relative to licking are on +11.0 ± 3.5 s on day 1, +0.6 ± 0.9 s on day 2 allowing for a single outlier, −5.1 ± 1.4 s on day 3 allowing for a single outlier, with $[DA]_{ex}$ now leading, and +22.8 ± 11.9 s on day 4. Impulses also lagged licking for randomly rewarded mice (+10.9 ± 7.9 s). A two-sample t test with respect to baseline animals yields $p = 0.04$ (day 2), $p = 0.005$ (day 3), $p = 0.9$ (day 4), and $p = 0.3$ (random); including the single outliers drops the evidence against a null hypothesis to $p = 0.6$ (day 2) and the still highly significant value $p = 0.02$ (day 3). The inset shows a scatterplot of the number of rewarded impulses versus lag time for individual mice on day 2 and day 3, together with a fit of the model (Equations 6 and 7 in STAR Methods) to the data.

(F) Standard boxplot shows the variance explained by an optimal linear filter that predicts licking from the measured $[DA]_{ex}$. "+" indicates an outlier that was not included in the mean. Solid bars indicate median. The values of R^2 for days 2 and 3 are significantly different than zero, with $p = 0.030$ and $p = 0.037$. The data for random reward, although very small at 0.019, are also significant ($p = 0.027$; $n = 12$) as a result of the large sample. Note 6-fold increase on 2nd day of feedback ON (day 3).

See also Figures S2 and S3.

the variance-explained (R^2), a metric for the strength of the predictability of licking from dopamine events. We found that there is a 6-fold increase in R^2 with feedback ON for day 3 compared to the case of random feedback (Figure 3F; cf. 3rd with 5th column). This increase in R^2 was absent when feedback was removed, i.e., feedback OFF on day 4 (Figure 3F; cf. 4th with 5th column).

Is there a theoretical means to understand how reinforcement can alter the rate and timing of stochastically occurring impulses of dopamine? We constructed a minimal theory that posits a generator of impulses and a hypothetical integrator of impulses above threshold (model in STAR Methods). The arrival of impulses is modeled as a shot effect with a Poisson rate and a stochastic distribution of amplitudes.[25,26] A set of coupled, leaky integrator equations ties the shift in lag time of impulses relative to a reward with the increase in rate of dopamine transients that may lead to impulses that cross a threshold. The model has two parameters that are numerically fit to data, i.e., a temporal scale for the impact of the lag time, which is fit with a full width at half maximum of 3 s, and a scale for the change in rate. We compared the predicted rate of rewarded impulses versus the lag time for the individually rewarded trains on day 2 and day 3 (inset in Figure 3E). The predicted relation, which is not monotonic, is in qualitative agreement with the data.

DISCUSSION

Dopamine is a ubiquitous neurotransmitter in the brain that signals many aspects of cognitive processing.[9] Early studies showed that a fraction of dopaminergic neurons in the midbrain produce impulses of spiking activity in response to a novel stimulus, even one that is not associated with a reward.[27] Further, such impulses may occur as a precursor to self-generated motion.[28,29] Most famously, unexpected rewards produce a transient increase in the spike rate of dopaminergic neurons that project to cortex and lead to increases in the concentration of $[DA]_{ex}$ in the midbrain and in cortex.[8] With repeated pairing of a neutral cue with a delayed reward, dopaminergic neurons shift their firing from the time of the reward to the time of the cue.[6,8] The increase in $[DA]_{ex}$ now represents the expectation of an upcoming reward, and the amplitude of this increase signals the probability of the reward.[9,20,30] A final twist is that the meaning of dopamine signals may change with experience.[31]

Here, we focused on the type of dopamine release in the cortex and report on a different behavior of dopamine impulses. In now classic literature, brief impulses of dopamine, in the context of Pavlovian conditioning, have been shown to represent reward prediction errors.[7] Notably, phasic dopamine firing and release advance in time from the presentation of reward to that of the earliest reward-predicting cue as animals learn to associate the cue with reward.[6,8] We observed spontaneous dopamine impulses in the absence of both sensory stimuli and reward in naive, head-fixed, awake animals on a treadmill. These dopamine impulses do not appear to report a reward prediction error, as there are no cues in the apparatus that would indicate the presence of reward. Furthermore, we find that these transients are not causally linked to the initiation of motor activity, i.e., licking or running (Figures 1C and 3F), as would be suggested by previous studies.[32,33] While we only measure licking and running behavior, it should be noted that dopamine appears to invigorate rather than initiate motor behavior,[33,34] and spontaneous motor behavior is, in fact, associated with a reduction in the firing rate of midbrain substantia nigra pars compacta neurons in the absence of cues or reward.[32,35]

The striatum receives extensive input from dopaminergic neurons from substantia nigra pars compacta and the ventral tegmentum area (VTA) of the basal ganglia. Past studies have almost exclusively focused on measuring dopamine dynamics of neurons in this region. However, anatomical studies have shown that a fraction of dopaminergic neurons in VTA project to all layers of somatosensory cortex, albeit with a bias to layer 5/6,[14] and that these neurons do not extend processes to striatum.[15] Furthermore, neurons in somatosensory cortex broadly express dopamine receptors; while the density of such receptors is highest in deep layers, a significant fraction of cells in the superficial layers express dopamine receptors.[36,37] Global activation of these receptors by the iontophoretic application of dopamine to somatosensory cortex leads to inhibition of activity in approximately half of the neurons measured.[38] Our work suggests the importance of further extending studies of dopamine dynamics to a cortical region with known plasticity.[11]

Our feedback scheme for reinforcement learning is modeled after schemes used in brain-machine interface (BMI) experiments.[39–41] Yet we did not supply cues related to the feedback signal other than the reward. In typical BMI experiments, animals are provided a real-time sensory feedback signal, e.g., an auditory tone,[41] that is modulated by the neuronal activity of interest. In particular, one BMI study found that animals were unable to modulate the neuronal activity toward the reward target in the absence of such cues.[41] In another study that involved learning to move a cursor based on neuronal activity in motor cortex, monkeys first needed to learn the task using their hands to control a physical joystick that moved a cursor on the screen. They then transferred this capability to pure control by neuronal activity. Unlike these BMI studies, we did not supply cues related to the feedback signal other than the reward (Figure 2A). Yet animals were able to perform our task and receive reward. This suggests that animals have an internal sense of $[DA]_{ex}$, most likely derived from the normal functioning of DA-GCPRs on cortical cells.

Our results highlight the potential role of internal brain dynamics in modulating as well as creating the spontaneous dopamine events. We observed that reinforcement learning may be used to train animals to initiate extrasynaptic impulses of dopamine in return for a reward (Figures 2 and 3). Pairing of a self-initiated increase of $[DA]_{ex}$ to a sucrose drop award is learned without a cue across two sessions (Figures 2B and 2C) and is readily unlearned and relearned across sessions (days 4 and 5 in Figure 2C). A minimal theory that posits a generator of impulses with stochastically assigned amplitudes and a hypothetical integrator of impulses above threshold can account for the data. These are judged to be physiologically plausible processes (inset in Figure 3E). We further conjecture that an animal's sense of spontaneous dopamine impulses may motivate it to search and forage in the absence of known reward-predictive

stimuli.[18,42] In this scenario, dopamine serves as a false, albeit stochastic, reward prediction error that motivates search through the role of dopamine as an anticipation signal for a future reward. Successful forages serve to amplify this motivational process. The broad temporal range of spontaneous events (Figures 1F and 3D) is consistent with search strategies.[43]

In contrast to dopamine impulses, tonic dopamine appears to affect how animals interact with their environment and explore. In particular, manipulations of tonic levels of $[DA]_{ex}$ modified how animals examined novel stimuli in various operant conditioning tasks[44–47] and the effort that animals were willing to exert to receive reward.[48,49] It is not clear whether tonic and phasic dopamine signals are independently controlled from one another.[50,51] A previous study[52] found that explicitly modeling tonic dopamine as a separate signal in the reward prediction error signal could reproduce the results of dopamine depletion on the response rate of rats rewarded on a fixed ratio reward schedule. While the authors used the average reward rate as an estimate of tonic dopamine, they note "...we should expect the tonic average reward signal to be used predictively and not only reactively, which would require it to be somewhat decoupled from the actual obtained phasic reward signal."[52] Therefore, our results suggest that tonic dopamine can be volitionally modulated independently of sensory stimuli.

A final point is that our focus has been on dopamine because of its well-known role in reward and prediction and the malleability of dopaminergic transmission with training. Yet our experiments do not speak to the possibility that other modulatory systems may also have spontaneous release in cortex. Other modulatory systems may be similarly or even more malleable in terms of volitional control of extrasynaptic neuromodulator concentration via feedback reinforcement training. The current results should be seen as a springboard to motivate and advance studies on the stochastic nature of neuromodulatory systems in general. In as much as the stochastic nature of synaptic release and that of random neuronal firing play a role in all aspects of brain function, including decision making, foraging, and attention,[53] the stochastic nature of neuromodulation may add a new dimension to brain dynamics.

STAR★METHODS

Detailed methods are provided in the online version of this paper and include the following:

- KEY RESOURCES TABLE
- RESOURCE AVAILABILITY
  - Lead contact
  - Materials availability
  - Data and code availability
- EXPERIMENTAL MODEL AND SUBJECT DETAILS
- METHOD DETAILS
  - Choice of dopamine indicator
  - Injection of mice for CNiFER measurements and/or $GRAB_{DA}$ expression
  - TPLSM imaging
  - Naive only
  - Adaptive threshold feedback training
  - MODEL
- QUANTIFICATION AND STATISTICAL ANALYSIS

SUPPLEMENTAL INFORMATION

Supplemental information can be found online at https://doi.org/10.1016/j.cub.2021.06.069.

ACKNOWLEDGMENTS

We thank Martin Deschênes for motivating our study; Winfried Denk, Michaël Elbaz, Michael Frank, Arif Hamid, Philbert Tsai, Bin Wang, and Fan Wang for discussions; Beth Friedman for comments on a draft; the late Roger Tsien for the gift of instruments used to assay the CNiFERs, and the National Institutes of Health (grants DA050159, DC009597, MH111499, NS107466, and NS097265) for funding.

AUTHOR CONTRIBUTIONS

C.F., D.K., P.A.S., and J.W.W. conceived the study. C.F. performed the experiments with the assistance of A.L., as well as performed the data analysis with input from D.K. J.A. devised the model, with input from C.F. and D.K. Reagents were supplied by D.K., Y.L., and P.A.S. D.K. finalized the manuscript with input from J.A., C.F., P.A.S., and J.W.W., as well as attended to the myriad of university rules and forms that govern environmental health and safety, including the ethical use of animals as well as the use of chemicals, controlled substances, hazardous substances, lasers, and viruses.

DECLARATION OF INTERESTS

The authors declare no competing interests.

Received: April 29, 2021
Revised: May 28, 2021
Accepted: June 24, 2021
Published: July 23, 2021

REFERENCES

1. Romo, R., and Schultz, W. (1990). Dopamine neurons of the monkey midbrain: contingencies of responses to active touch during self-initiated arm movements. J. Neurophysiol. *63*, 592–606.
2. Phillips, P.E.M., Stuber, G.D., Heien, M.L.A.V., Wightman, R.M., and Carelli, R.M. (2003). Subsecond dopamine release promotes cocaine seeking. Nature *422*, 614–618.
3. Collins, A.L., Greenfield, V.Y., Bye, J.K., Linker, K.E., Wang, A.S., and Wassum, K.M. (2016). Dynamic mesolimbic dopamine signaling during action sequence learning and expectation violation. Sci. Rep. *6*, 20231.
4. Howe, M.W., Tierney, P.L., Sandberg, S.G., Phillips, P.E.M., and Graybiel, A.M. (2013). Prolonged dopamine signalling in striatum signals proximity and value of distant rewards. Nature *500*, 575–579.
5. Hamid, A.A., Pettibone, J.R., Mabrouk, O.S., Hetrick, V.L., Schmidt, R., Vander Weele, C.M., Kennedy, R.T., Aragona, B.J., and Berke, J.D. (2016). Mesolimbic dopamine signals the value of work. Nat. Neurosci. *19*, 117–126.
6. Muller, A., Joseph, V., Slesinger, P.A., and Kleinfeld, D. (2014). Cell-based reporters reveal in vivo dynamics of dopamine and norepinephrine release in murine cortex. Nat. Methods *11*, 1245–1252.
7. Schultz, W. (2015). Neuronal reward and decision signals: from theories to data. Physiol. Rev. *95*, 853–951.
8. Schultz, W., Apicella, P., and Ljungberg, T. (1993). Responses of monkey dopamine neurons to reward and conditioned stimuli during successive steps of learning a delayed response task. J. Neurosci. *13*, 900–913.
9. Schultz, W., Dayan, P., and Montague, P.R. (1997). A neural substrate of prediction and reward. Science *275*, 1593–1599.

10. Diamond, M.E., Huang, W., and Ebner, F.F. (1994). Laminar comparison of somatosensory cortical plasticity. Science *265*, 1885–1888.
11. Feldman, D.E. (2000). Timing-based LTP and LTD at vertical inputs to layer II/III pyramidal cells in rat barrel cortex. Neuron *27*, 45–56.
12. Svoboda, K., Denk, W., Kleinfeld, D., and Tank, D.W. (1997). *In vivo* dendritic calcium dynamics in neocortical pyramidal neurons. Nature *385*, 161–165.
13. Drew, P.J., Shih, A.Y., Driscoll, J.D., Knutsen, P.M., Blinder, P., Davalos, D., Akassoglou, K., Tsai, P.S., and Kleinfeld, D. (2010). Chronic optical access through a polished and reinforced thinned skull. Nat. Methods *7*, 981–984.
14. Descarries, L., Lemay, B., Doucet, G., and Berger, B. (1987). Regional and laminar density of the dopamine innervation in adult rat cerebral cortex. Neuroscience *21*, 807–824.
15. Aransay, A., Rodríguez-López, C., García-Amado, M., Clascá, F., and Prensa, L. (2015). Long-range projection neurons of the mouse ventral tegmental area: a single-cell axon tracing analysis. Front. Neuroanat. *9*, 59.
16. Quintana, C., and Beaulieu, J.-M. (2019). A fresh look at cortical dopamine D2 receptor expressing neurons. Pharmacol. Res. *139*, 440–445.
17. Threlfell, S., Lalic, T., Platt, N.J., Jennings, K.A., Deisseroth, K., and Cragg, S.J. (2012). Striatal dopamine release is triggered by synchronized activity in cholinergic interneurons. Neuron *75*, 58–64.
18. Mohebi, A., Pettibone, J.R., Hamid, A.A., Wong, J.T., Vinson, L.T., Patriarchi, T., Tian, L., Kennedy, R.T., and Berke, J.D. (2019). Dissociable dopamine dynamics for learning and motivation. Nature *570*, 65–70.
19. Patriarchi, T., Cho, J.R., Merten, K., Howe, M.W., Marley, A., Xiong, W.H., Folk, R.W., Broussard, G.J., Liang, R., Jang, M.J., et al. (2018). Ultrafast neuronal imaging of dopamine dynamics with designed genetically encoded sensors. Science *360*, e6396.
20. Sun, F., Zeng, J., Jing, M., Zhou, J., Feng, J., Owen, S.F., Luo, Y., Li, F., Wang, H., Yamaguchi, T., et al. (2018). A genetically encoded fluorescent sensor enables rapid and specific detection of dopamine in flies, fish, and mice. Cell *174*, 481–496.e19.
21. Nguyen, Q.-T., Schroeder, L.F., Mank, M., Muller, A., Taylor, P., Griesbeck, O., and Kleinfeld, D. (2010). An *in vivo* biosensor for neurotransmitter release and *in situ* receptor activity. Nat. Neurosci. *13*, 127–132.
22. Sutton, R.S., and Barto, A.G. (1998). Reinforcement Learning: An Introduction (MIT).
23. Seung, H.S. (2003). Learning in spiking neural networks by reinforcement of stochastic synaptic transmission. Neuron *40*, 1063–1073.
24. Leek, M.R. (2001). Adaptive procedures in psychophysical research. Percept. Psychophys. *63*, 1279–1292.
25. Kingman, J.F.C. (1993). Poisson Processes (Clarendon).
26. Richardson, M.J.E., and Swarbrick, R. (2010). Firing-rate response of a neuron receiving excitatory and inhibitory synaptic shot noise. Phys. Rev. Lett. *105*, 178102.
27. Schultz, W., and Romo, R. (1990). Dopamine neurons of the monkey midbrain: contingencies of responses to stimuli eliciting immediate behavioral reactions. J. Neurophysiol. *63*, 607–624.
28. Horvitz, J.C., Stewart, T., and Jacobs, B.L. (1997). Burst activity of ventral tegmental dopamine neurons is elicited by sensory stimuli in the awake cat. Brain Res. *759*, 251–258.
29. Coddington, L.T., and Dudman, J.T. (2019). Learning from action: reconsidering movement signaling in midbrain dopamine neuron activity. Neuron *104*, 63–77.
30. Glimcher, P.W. (2011). Understanding dopamine and reinforcement learning: the dopamine reward prediction error hypothesis. Proc. Natl. Acad. Sci. USA *108* (*Suppl 3*), 15647–15654.
31. Engelhard, B., Finkelstein, J., Cox, J., Fleming, W., Jang, H.J., Ornelas, S., Koay, S.A., Thiberge, S.Y., Daw, N.D., Tank, D.W., and Witten, I.B. (2019). Specialized coding of sensory, motor and cognitive variables in VTA dopamine neurons. Nature *570*, 509–513.
32. Coddington, L.T., and Dudman, J.T. (2018). The timing of action determines reward prediction signals in identified midbrain dopamine neurons. Nat. Neurosci. *21*, 1563–1573.
33. Howe, M.W., and Dombeck, D.A. (2016). Rapid signalling in distinct dopaminergic axons during locomotion and reward. Nature *535*, 505–510.
34. da Silva, J.A., Tecuapetla, F., Paixão, V., and Costa, R.M. (2018). Dopamine neuron activity before action initiation gates and invigorates future movements. Nature *554*, 244–248.
35. Dodson, P.D., Dreyer, J.K., Jennings, K.A., Syed, E.C.J., Wade-Martins, R., Cragg, S.J., Bolam, J.P., and Magill, P.J. (2016). Representation of spontaneous movement by dopaminergic neurons is cell-type selective and disrupted in parkinsonism. Proc. Natl. Acad. Sci. USA *113*, E2180–E2188.
36. Ariano, M.A., and Sibley, D.R. (1994). Dopamine receptor distribution in the rat CNS: elucidation using anti-peptide antisera directed against D1A and D3 subtypes. Brain Res. *649*, 95–110.
37. Yu, Q., Liu, Y.-Z., Zhu, Y.-B., Wang, Y.-Y., Li, Q., and Yin, D.M. (2019). Genetic labeling reveals temporal and spatial expression pattern of D2 dopamine receptor in rat forebrain. Brain Struct. Funct. *224*, 1035–1049.
38. Bassant, M.H., Ennouri, K., and Lamour, Y. (1990). Effects of iontophoretically applied monoamines on somatosensory cortical neurons of unanesthetized rats. Neuroscience *39*, 431–439.
39. Fetz, E.E. (1969). Operant conditioning of cortical unit activity. Science *163*, 955–958.
40. Nicolelis, M.A.L., and Lebedev, M.A. (2009). Principles of neural ensemble physiology underlying the operation of brain-machine interfaces. Nat. Rev. Neurosci. *10*, 530–540.
41. Neely, R.M., Koralek, A.C., Athalye, V.R., Costa, R.M., and Carmena, J.M. (2018). Volitional modulation of primary visual cortex activity requires the basal ganglia. Neuron *97*, 1356–1368.e4.
42. Berridge, K.C., and Robinson, T.E. (1998). What is the role of dopamine in reward: hedonic impact, reward learning, or incentive salience? Brain Res. Brain Res. Rev. *28*, 309–369.
43. Sims, D.W., Humphries, N.E., Hu, N., Medan, V., and Berni, J. (2019). Optimal searching behaviour generated intrinsically by the central pattern generator for locomotion. eLife *8*, e50316.
44. Dulawa, S.C., Grandy, D.K., Low, M.J., Paulus, M.P., and Geyer, M.A. (1999). Dopamine D4 receptor-knock-out mice exhibit reduced exploration of novel stimuli. J. Neurosci. *19*, 9550–9556.
45. Cinotti, F., Fresno, V., Aklil, N., Coutureau, E., Girard, B., Marchand, A.R., and Khamassi, M. (2019). Dopamine blockade impairs the exploration-exploitation trade-off in rats. Sci. Rep. *9*, 6770.
46. Costa, V.D., Tran, V.L., Turchi, J., and Averbeck, B.B. (2014). Dopamine modulates novelty seeking behavior during decision making. Behav. Neurosci. *128*, 556–566.
47. Zhuang, X., Oosting, R.S., Jones, S.R., Gainetdinov, R.R., Miller, G.W., Caron, M.G., and Hen, R. (2001). Hyperactivity and impaired response habituation in hyperdopaminergic mice. Proc. Natl. Acad. Sci. USA *98*, 1982–1987.
48. Aberman, J.E., and Salamone, J.D. (1999). Nucleus accumbens dopamine depletions make rats more sensitive to high ratio requirements but do not impair primary food reinforcement. Neuroscience *92*, 545–552.
49. Beeler, J.A., Daw, N., Frazier, C.R.M., and Zhuang, X. (2010). Tonic dopamine modulates exploitation of reward learning. Front. Behav. Neurosci. *4*, 170.
50. Floresco, S.B., West, A.R., Ash, B., Moore, H., and Grace, A.A. (2003). Afferent modulation of dopamine neuron firing differentially regulates tonic and phasic dopamine transmission. Nat. Neurosci. *6*, 968–973.
51. Berke, J.D. (2018). What does dopamine mean? Nat. Neurosci. *21*, 787–793.

52. Niv, Y., Daw, N.D., Joel, D., and Dayan, P. (2007). Tonic dopamine: opportunity costs and the control of response vigor. Psychopharmacology (Berl.) *191*, 507–520.

53. Deco, G., Rolls, E.T., and Romo, R. (2009). Stochastic dynamics as a principle of brain function. Prog. Neurobiol. *88*, 1–16.

54. Tsai, P.S., and Kleinfeld, D. (2009). Methods for In Vivo Optical Imaging, Second Edition, R.D. Frostig, ed. (CRC), pp. 59–115.

55. Aljadeff, J., Lansdell, B.J., Fairhall, A.L., and Kleinfeld, D. (2016). Analysis of neuronal spike trains, deconstructed. Neuron *91*, 221–259.

56. Percival, D.B., and Walden, A.T. (1993). Spectral Analysis for Physical Applications: Multitaper and Conventional Univariate Techniques (Cambridge University).

57. Mitra, P.P., and Bokil, H.S. (2008). Observed Brain Dynamics (Oxford University).

STAR★METHODS

KEY RESOURCES TABLE

REAGENT or RESOURCE	SOURCE	IDENTIFIER
Bacterial and virus strains		
AAV-hSyn-DA4.4	Yulong Li Laboratory	N/A
Chemicals, peptides, and recombinant proteins		
Isoflurane	Henry Schein	Cat. No. 1182097
Buprenorphine Hydrochloride, Injection	MWI Veterinary Supply	Cat. No. 60969
Cyclosporine	Teva Generics	Cat. No. 00093-5742-65
Sucrose	Sigma Aldrich	Cat. No. S0389
Experimental models: cell lines		
Human: Cell line HEK293: M1-CNiFER	David Kleinfeld Laboratory	N/A
Human: Cell line HEK293: D2-CNiFER	David Kleinfeld Laboratory	N/A
Experimental models: organisms/strains		
Mouse: C57BL/6J	The Jackson Laboratory	RRID: IMSR_JAX:000664
Software and algorithms		
MATLAB	MathWorks	RRID: SCR_001622
ScanImage	Vidrio	RRID: SCR_014307
Chronux	Cold Spring Harbor Laboratory	RRID: SCR_005547
Other		
Optical Lickometer	Sanworks	Cat. No. 1020
Rotary Encoder	Koyo Electronics	Cat. No. TRD-S360BD
National Instruments USB board	National Instruments	Cat. No. USB-6211
PowerLab/8SP	AD Instruments	RRID: SCR_018833
Solenoid Valve	Parker Instrumentation	Cat. No. 003-0137-900

RESOURCE AVAILABILITY

Lead contact

Further information and requests for resources and reagents should be directed to and will be fulfilled by Dr. David Kleinfeld (dk@physics.ucsd.edu).

Materials availability

This study did not generate new unique reagents.

Data and code availability

The datasets supporting the current study, and an associated "read me" file, are available at https://datadryad.org/stash/share/He3oAHCTB6W0fUlaULv2i-WtySJu3LqkQJavqKsLBSo.

The code for the model is available at https://github.com/aljdf/DopamineTransients_Foo2021.

EXPERIMENTAL MODEL AND SUBJECT DETAILS

The Institutional Animal Care and Use Committee at the University of California San Diego approved all protocols. Adult, male C57BL/6 mice, age P30 to P45, were maintained in standard cages on a natural light-dark cycle. For surgery, mice were anesthetized with isoflurane (Butler Schein). Body temperature was monitored and maintained at 37°C. Subcutaneous injections of 5% (w/v) glucose in saline were given every 2 h for rehydration. Buprenorphine (0.02 mg/kg, Butler Schein) was administered i.p. for post-operative analgesia.

METHOD DETAILS

Choice of dopamine indicator

CNiFERs are dual-wavelength sensors. This helps ensure that our measurements were relatively insensitive to motion and bleaching of fluorophores. D2-CNiFERs provide sensitivity from $[DA]_{ex}$ »2 to 200 nM and have a 2 s temporal resolution.[6] While single-wavelength genetically-encoded fluorescent probes whose optical properties depend on $[DA]_{ex}$, have been developed,[19,20] these are all single wavelength so that it is difficult to compensate for drift. Further, we found that the signal from a current single-wavelength sensor substantially diminished over the multi-day period of our experiments, while that from CNiFERs was stable (Figure S1).

Injection of mice for CNiFER measurements and/or $GRAB_{DA}$ expression

CNiFER cells were implanted for imaging as described.[6] $GRAB_{DA}$ expression was induced by injection of 0.5 - 1.0 uL of 10^{13} μg/ml of an AAV2 virus containing the $GRAB_{DA}$ sequence under the synapsin promoter.[20] The injections were made in frontal somatosensory cortex, 1.5 M/L, 1.5 R/C using a quartz glass pipette. At least three weeks were allowed for expression of the virus. A thin skull craniotomy[13] was made for animals that did not express $GRAB_{DA}$, whereas an open craniotomy was made for animals that expressed $GRAB_{DA}$. The craniotomies were 3 - 4 mm in diameter. In $GRAB_{DA}$ expressing animals, CNiFER cells were injected as close as possible to the $GRAB_{DA}$ expression area without overlapping or rupturing pial vessels, typically 60 - 100 μm away.

TPLSM imaging

In vivo imaging[12] was performed with a custom-built two-photon laser-scanning microscope.[54] Two-photon imaging was need to image through the thin skull to minimize the potential for inflammation consistent with high signal to noise ratio.[13] Control of scanning and data acquisition was achieved through the ScanImage software platform (Vidrio). Excitation light at 840 nm was used to excite the CFP portion of TN-XXL. Fluorescence was collected by a 25X dipping objective (HCX-IRAPO, Leica). The fluorescent signal was split into two channels using a 506 nm long-pass dichroic mirror. Each channel was further bandpass filtered: 465 ± 20 nm for measurement of emission by CFP ($F_{465\ nm}$) and 520 ± 20 nm for emission by YFP ($F_{520\ nm}$) and the change in FRET signal, denoted ΔR(t)/R, was calculated as

$$\frac{\Delta R(t)}{R} = \frac{F_{520\ nm}(t)/F_{520\ nm}}{F_{465\ nm}(t)/F_{465\ nm}} - 1 \qquad \text{(Equation 1)}$$

where á$F_{520\ nm}$ñ and á$F_{465\ nm}$ñ refer to the baseline values determined from a LOWESS fit (see Quantification and statistical analysis). Running activity was recorded using a rotary encoder (TRD-S360BD, Koyo Electronics) attached to the underside of a rotation platform (Figures 2A and 3A). Licking activity was recorded using an optical lickometer (Sanworks LLC). The analog signals were recorded using a PowerLab 8.35 device (ADInstruments) acquiring at 1 kHz and synchronized with the two-photon imaging data using the frame trigger output of ScanImage.

Naive only

After one day of recovery from surgery, mice were water deprived (24h/day). Imaging began the following day. The animals were placed in a stationary head-frame fixed on top of a wheel; no lick port pas present nor was a reward or cues were given. The animals were allowed to locomote freely. Each imaging session lasted for one hour, after which the animals were returned to their home cages. Animals were given unrestricted access to water for one hour after imaging. Animals were imaged under identical conditions for four successive days.

Adaptive threshold feedback training

After one day of recovery from surgery, mice were water deprived (24h/day). Imaging began the following day. During the first day of imaging, the animals were placed in a stationary head-frame fixed on top of a wheel with a lick port. No reward or cues were given, and the animals were allowed to lick and run freely. For imaging trials with feedback reinforcement, animals were placed in the same head-frame, but given a reward, 0.1 mL of 10% (v/v) sucrose water, for increasing their measured neuromodulator concentration. Real-time readout of neuromodulator concentration and reward administration were done using custom written ScanImage user functions. Each imaging session lasted for one hour, after which the animals were returned to their home cages. Animals were given unrestricted access to water for one hour after imaging. Animals were imaged once a day for 4 - 6 consecutive days, depending on the optical quality of the CNiFER implants.

Rewards were dispensed using a gravity fed solenoid (VAC-100 PSIG, Parker Instrumentation) system. A 50 mL reservoir of 10% (v/v) sucrose water was hung from a stand, and a solenoid was used to control the flow of liquid coming out of the reservoir. The output of this solenoid was routed to the input of the lick port. A second solenoid controlled the vacuum which was connected to the output of the lick port. The timing and control of both solenoids used a National Instruments board (USB-6211, National Instruments) interfaced with ScanImage. The initial threshold for reward was determined by taking 80% of the average amplitude of spontaneous neuromodulator transients from the first day of imaging data, and the threshold increment was 50% of this initial reward threshold. Reward administration occurred 0.25 s after the detection of the neuromodulator concentration rising above the threshold level, with a minimum delay of 3.5 s between rewards. At a time of 0.5 s after reward administration, a vacuum was activated for 1 s to remove any leftover sucrose water. The reward threshold was increased by the threshold increment whenever a reward was

administered. If animals did not receive a reward within 225 s of the previous reward, the reward threshold was decreased by the threshold increment, down to a minimum of the initial threshold.

MODEL

To study the learning dynamics related to stochastic dopamine impulses, we built a phenomenological model of the dopamine transients and their relationship to reward seeking behavior, i.e., licking. In our model, the dopamine concentration, denoted *D(t)* in the equations rather than the observed $[DA]_{ex}$, are taken as a shot noise process. Here, pulses of dopamine follow a Poisson process with rate λ; they decay with timescale τ; and the average amplitude of discrete jumps in *D(t)* is *A*. For mathematical tractability we assume the amplitude of each pulse follows an exponential distribution. We write

$$\tau \frac{d}{dt} D(t) = -D(t) + \sum_k a_k \delta(t - t_k), \quad \text{(Equation 2)}$$

where t_k is the time of impulse *k*, $a_k \sim Exp(\mathrm{A})$, and $\delta(\cdot)$ is the Dirac delta function. At steady-state, the dopamine concentrations follow a gamma distribution for this process[25,26]

$$\mathrm{P}(D) = \frac{D^{\tau\lambda - 1}}{\Gamma(\tau\lambda) A^{\tau\lambda}} e^{-\mathrm{D}/A}, \quad \text{(Equation 3)}$$

The probability that the dopamine concentration lies above a threshold, denoted θ, is then

$$\mathrm{P}(D > \theta) = \int_\theta^\infty dD\, P(D) = \frac{\gamma(\tau\lambda, \theta/\mathrm{A})}{\Gamma(\tau\lambda)}, \quad \text{(Equation 4)}$$

where we have used $\Gamma(\cdot)$ for the gamma function and $\gamma(\cdot,\cdot)$ for the incomplete gamma function.

Next we consider the effect of transiently crossing threshold on the rate of dopamine pulses. We assume that there is some stable steady state rate of pulses, denoted λ_0. When the transient dopamine exceeds a threshold, the rate is increased by an amount λ_1, if the pulse arrives in close proximity to a reward. We denote the lag between dopamine pulse and reward by Δ and the width of the learning window by Δ_w. The equation for the change in the dopamine pulse rate reads

$$\frac{d}{dt}\lambda(t) \propto (\lambda_0 - \lambda) + \lambda_1 \Theta(D - \theta)\, e^{-|\Delta|/\Delta_w}, \quad \text{(Equation 5)}$$

where $\Theta(\cdot)$ is the Heaviside function. We are interested in the steady state behavior of the system, so the timescale of changes in λ, i.e., the proportionality constant in Equation 5, will not enter our analysis.

We similarly assume that the delay Δ relaxes to a baseline value Δ_0 and that every time the dopamine exceeds threshold it changes by some amount Δ_1. This gives,

$$\frac{d}{dt}\Delta(t) \propto (\Delta_0 - \Delta) + \Delta_1 \Theta(D - \theta) \quad \text{(Equation 6)}$$

At steady state we set all time-derivatives to zero and use the probability of exceeding threshold to obtain,

$$\Delta = \Delta_0 + \Delta_1 \frac{\gamma(\tau\lambda, \theta/A)}{\Gamma(\tau\lambda)} \quad \text{(Equation 7)}$$

and

$$\lambda = \lambda_0 + \lambda_1 \frac{\gamma(\tau\lambda, \theta/A)}{\Gamma(\tau\lambda)}\, e^{-\left|\Delta_0 + \Delta_1 \frac{\gamma(\tau\lambda, \theta/A)}{\Gamma(\tau\lambda)}\right| \Big/ \Delta_w} \quad \text{(Equation 8)}$$

Equation 8 is a nonlinear equation for the rate of dopamine impulses at steady state as a function of itself, the model parameters, and the threshold θ. We stress that θ should be related to, but is not identical to, the threshold on dopamine set experimentally. The reason is that that threshold changes transiently during learning, and the experiments include baseline changes of the dopamine concentration that are beyond the scope of the model. We therefore solve the equation for λ numerically over a broad range of values for θ. Once $\lambda = \lambda(\theta)$ is obtained, we compute $\Delta = \Delta(\lambda, \theta)$ by substituting into Equation 7.

We are interested in the qualitative behavior of the model. Thus four of the six parameters were chosen based on averaging the experimental results over animals without studying the effects of varying the parameter systematically. Specifically, we set λ_0 = 0.01 Hz (Figure 1D), τ = 30 s (Figure 1E), Δ_0 = 5 s (Figure 3E), and $\Delta_1 = -21$ s (Figure 3E); the final assignment is based on the argument that if threshold is exceeded "easily," the dopamine pulse rate will decay to Δ_0 - Δ_1 (Equation 6). The earliest delay we measured for an animal averaged over one day of the experiment was -16 s, so we set $\Delta_1 = -21$ s. This parameter choice is based on the animal with largest delay since we want the model to apply to all animals during the closed loop learning of Day 2 and Day 3. The remaining two parameters, λ_1 and Δ_w, were fit numerically to data. We focused on positive values of λ_1 because the dopamine rate increases when threshold is crossed, although nontrivial solutions of Equation 7 exist when λ_1 is negative.

We fit the parameters (Δ_ω, λ_1) across the dataset of each animal at Day 2 and Day 3 (insert, Figure 3E) by minimizing the sum of the squared error over all data. We used 1000 values of θ between 10^{-7} and 10^3 that were equally spaced on a logarithmic scale. The lowest sum of squared errors was found for $\Delta_w = 1.6$ s and $\lambda_1 = 0.087$ Hz. We note that for some value of the parameters the solution of $\lambda = \lambda(\Delta)$ is discontinuous, i.e., for some values of Δ there is no corresponding rate λ that solves Equation 8. For the purposes of fitting we linearly interpolated $\lambda = \lambda(\Delta)$ between the points of discontinuity since the model equations are solved at steady-state while individual animals are measured during the transient process of learning (interpolation indicated by dashed line in inset to Figure 3E).

QUANTIFICATION AND STATISTICAL ANALYSIS

All data analysis was done using MATLAB. TN-XXL fluorescence traces were normalized to baseline intensities measured from an initial period of 600 s at the beginning of each imaging trial during which no reward was given. The neuromodulator concentration was calculated as the fractional change in the FRET ratio.[6] The FRET response was separated into a baseline and phasic component by performing a LOWESS fit on the data using a window size of 470 s and a step size of 4.7 s. The fitted curve was defined as the baseline (low-frequency) component, and the residual (high-frequency) was defined as the transient component. $GRAB_{DA}$ fluorescence traces were also normalized to baseline intensities measured from the initial 600 s period without reward. Baseline trends in the $GRAB_{DA}$ fluorescence traces were corrected using the same method as the FRET response; a LOWESS fit using the same parameters was subtracted from the trace and the residual was used.

Licks were detected from the lickometer data by low pass filtering the lickometer signal, subtracting a 3-sample median filter of the signal and detecting the subsequent rising edges. The licking frequency was calculated by taking a 1 s window around the sample point and counting the number of licks in the window. Running speed was similarly calculated from the encoder signal by detecting both rising and falling edges and counting the number of edges in a 0.235 s window around the sample point.

Significant transient were detected from the transient component of the FRET response as those epochs whose amplitude exceeded 2-times the root-mean-square level of the noise. The amplitude was calculated as the maximum value in each detected transient epoch, and the width was the full width at half maximum amplitude (FWHM) of the transient.

The onset of neuromodulator transients was defined as the point at which the ratio $\Delta R/R$ increased by 2-times the root-mean-square level of the baseline noise. The onsets of licking and running bouts were calculated in a similar manner. Onset times were calculated separately for each imaging trial from the average transient-triggered response. The lags of the FRET signal behind the licking and running signals were defined as the difference in the onset time.

All statistics were calculated with a one-sided Student's t test. Standard box plots were used; the box held the middle quartiles, the colored line indicates the median value, the whiskers denote the full range of the data except for outliers, which are determined by Chauvener's criterion and shown as separate points.
A linear model was used to fit the FRET response to the licking and running traces.[55] The transfer function of the model was calculated directly from the power spectra of the respective traces as the cross power divided by the input power. New models were fit for each imaging trial, and the variance explained, i.e., R^2, was calculated directly from the predicted FRET. Spectral power density and spectral coherence were calculated using multi-taper methods[56] with a time-bandwidth product of 10 and the Chronux package.[57]